Published in final edited form as:
J Neurosci Res. 2009 September ; 87(12): 2728–2739. doi:10.1002/jnr.22089.

Mitochondrial Inhibitor 3-Nitroproprionic Acid Enhances Oxidative Modification of Alpha-synuclein in a Transgenic Mouse Model of Multiple System Atrophy

Kiren Ubhi[1], **Phil Hyu Lee**[2], **Anthony Adame**[1], **Chandra Inglis**[1], **Michael Mante**[1], **Edward Rockenstein**[1], **Nadia Stefanova**[3], **Gregor K. Wenning**[3], and **Eliezer Masliah**[1,4,*]

[1]Department of Neurosciences, School of Medicine, University of California–San Diego, La Jolla, California

[2]Department of Neurology, Yonsei University College of Medicine, Seoul, South Korea

[3]Clinical Neurobiology Section, Department of Neurology, Innsbruck Medical University, Innsbruck, Austria

[4]Department of Pathology, School of Medicine, University of California–San Diego, La Jolla, California

Abstract

Multiple system atrophy (MSA) is a progressive neurodegenerative disease characterized by autonomic failure, parkinsonism, cerebellar ataxia, and oligodendrocytic accumulation of alpha-synuclein (αsyn). Oxidative stress has been linked to neuronal death in MSA and the mitochondrial toxin 3-nitropropionic acid (3NP) is known to enhance the motor deficits and neurodegeneration in transgenic mice models of MSA. However, the effect of 3NP administration on αsyn itself has not been studied. In this context, we examined the neuropathological effects of 3NP administration in αsyn transgenic mice expressing human αsyn (hαsyn) under the control of the myelin basic protein (MBP) promoter and the effect of this administration on posttranslational modifications of αsyn, on levels of total αsyn, and on its solubility. We demonstrate that 3NP administration altered levels of nitrated and oxidized αsyn in the MBP-hαsyn tg while not affecting global levels of phosphorylated or total αsyn. 3NP administration also exaggerated neurological deficits in the MBP-hαsyn tg mice, resulting in widespread neuronal degeneration and behavioral impairment.

Keywords

behavior; oligodendrocytes; synucleinopathy

Multiple system atrophy (MSA) is a sporadic neurodegenerative disease of the central and autonomic nervous system. Cardinal clinical features include autonomic failure, parkinsonism, cerebellar ataxia, and pyramidal signs (Wenning et al., 2004). Pathologically, MSA is primarily characterized by alpha-synuclein (αsyn)-positive glial cytoplasmic inclusions, although αsyn inclusions in neurons have also been reported. Neuronal loss, predominantly in the basal ganglia, brain stem, and cerebellum is also a key pathological feature of MSA (Burn and Jaros, 2001). Currently there are no therapeutic treatments for MSA, and although patients are

*Correspondence to: Eliezer Masliah, Department of Neurosciences, University of California–San Diego, La Jolla, CA 92093-0624. emasliah@ucsd.edu.
The first two authors contributed equally to this work.

prescribed drugs to manage the symptoms of MSA, these do nothing to halt the progression of the disease or tackle the underlying cause.

Although the exact mechanisms underlying the abnormal accumulation and aggregation of αsyn in MSA remain unclear, evidence from case–control epidemiological studies suggests that occupational exposure to pesticides, insecticides, or chemicals interfering with the mitochondrial electron transport chain may be associated with increased risk of MSA (Hanna et al., 1999; Nee et al., 1991; Vanacore et al., 2005). In animal studies, chronic administration of 3-nitropropionic acid (3NP), an environmental toxin that inhibits mitochondrial complex II function, has been reported to mimic MSA (Stefanova et al., 2005b). Furthermore, high doses of 3NP, although eventually leading to significant mortality in treated mice, have been demonstrated to aggravate nigrostriatal and olivopontocerebellar degeneration in MSA transgenic mice expressing αsyn under the control of the oligodendrocytic proteolipid promoter (Stefanova et al., 2005a). Results from these studies highlight the role of mitochondrial dysfunction and oxidative stress as risk factors triggering or exaggerating MSA pathology.

Despite the ability of 3NP administration to exacerbate MSA-like pathology in transgenic mice models, little is known about the effect of 3NP administration on the expression of αsyn itself, specifically in relation to posttranslational modifications of αsyn. In this context, we administered low-dose 3NP to mice expressing αsyn under the myelin basic protein (MBP) promoter to investigate how 3NP administration would affect levels of total, phosphorylated, nitrated, and oxidized αsyn and αsyn solubility.

We found that administration of the mitochondrial inhibitor 3NP results in oxidative modifications to αsyn, as evidenced by the immunoblot and immunohistochemical analysis of nitrated and oxidized αsyn. The increased levels of oxidized αsyn observed in the 3NP-treated MBP–human αsyn (hαsyn) mice were accompanied by an exacerbation of behavioral deficits and pathology in the brain regions affected in patients with MSA.

Materials and Methods

Animals and Treatment

The generation and characterization of the MBP human αsyn transgenic (MBP-hαsyn tg) mice has been previously described (Shults et al., 2005). In the present study, we used a total of 24 mice with a mean age of 8.9 months. Mice of each genotype (MBP hαsyn tg [n = 12] or nontransgenic littermates [NTg] [n = 12]) were divided into saline- and 3NP-treated groups. 3NP was dissolved in saline and pH 7.4 was adjusted with 1 mol/L NaOH. The 3NP (or saline) was administrated intraperitoneally twice daily over 6 days according to the following dosage protocol: 10 mg/kg (days 1 and 2), 20 mg/kg (day 3 and 4), and 30 mg/kg (days 5 and 6), total dose 290 mg/kg in 6 days. Behavioral analysis was conducted 3 weeks after the final injection, and mice were killed immediately after behavioral testing.

Tissue Processing

Following the National Institutes of Health guidelines for the humane treatment of animals, under anesthesia, mice were killed and brains removed. The right hemibrain was immersion-fixed in 4% paraformaldehyde in pH 7.4 phosphate-buffered saline and serially sectioned at 40 μm with a Vibratome (Leica, Deerfield, IL). The left hemibrain was kept at −80°C for biochemical analysis.

Western Blot Analysis

Protein levels of total, phosphorylated (S129), nitrated, and oxidized αsyn were determined by immunoblot analysis. Fractional analysis of hαsyn accumulation was performed as described

previously (Kahle et al., 2002; Shults et al., 2005). Briefly, hemibrains were sonicated in tris-buffered saline plus protease inhibitor (TBS+) (Sigma, St. Louis, MO) and centrifuged for 5 min at 1,000*g*, and the resulting supernatants were ultracentrifuged for 1 hr at 130,000*g*. The supernatants from this step represented the TBS-soluble fractions. Pellets were then rinsed twice with TBS1 and extracted with 500 μl of 5% sodium dodecyl sulfate (SDS) in TBS+ and ultracentrifuged for 30 min at 130,000*g*, and the pellets were reextracted twice, collecting the detergent-soluble supernatants (SDS-soluble fraction). The detergent-insoluble pellets were squashed in 100 μl of 8 M urea/5% SDS in TBS+ and incubated for 10 min at room temperature. Eighty microliters of the resulting suspension was mixed with 20 μl of trichloroacetic acid and allowed to precipitate overnight at 4°C, and precipitates were collected in protein gel-loading buffer containing 5.3 M urea. For TBS- and SDS-soluble fractions, 15 μg of protein was loaded for each lane. For urea extract, all protein precipitates in each sample were loaded. Membranes were probed with primary antibodies for polyclonal αsyn (1:1,000; Chemicon, Temecula, CA), phosphorylated Ser-129-specific αsyn 11A5 (1:250, Kahle et al., 2002), nitrated αsyn (1:1,000, Upstate, Lake Placid, NY), and oxidized αsyn (Syn 514, 1:1,000, Abcam, Cambridge, MA). Anti-β-actin (1:1,000, Sigma, CA) was used to confirm equal loading. After overnight incubation with primary antibodies, membranes were incubated in appropriate secondary antibodies, reacted with enhanced chemiluminescence, and developed on a VersaDoc gel-imaging machine (Bio-Rad, Hercules, CA).

Immunohistochemistry and Image Analysis

Vibratome sections (40 μm thick) were immunolabeled overnight with antibodies against αsyn (1:1,000, Chemicon), phosphorylated αsyn (1:1,000, Millipore), nitrated αsyn (1:1,000, Millipore), the neuronal marker NeuN (1:1,000, Chemicon), tyrosine hydroxylase (TH, 1:1,000, Millipore), and adenomatous polyposis coli (APC, 1:1,000, Abcam). The next day, sections were incubated with species-appropriate biotinylated secondary antibodies (1:200, Vector Laboratories) and avidin D–horseradish peroxidase (1:200; ABC Elite; Vector Laboratories), and reacted with diaminobenzidine tetrahydrochloride containing 0.001% H_2O_2. To assess apoptosis, sections were double-labeled with a monoclonal antibody against activated caspase 3 (1:200, Stressgen Bioreagents, Ann Arbor, MI) and an antibody against αsyn (1:1,000, Chemicon), followed by incubation with fluorochrome-labeled secondary antibodies. The immunolabeled blind-coded sections were analyzed on a bright-field microscope, and images were captured with a digital camera.

Stereological Analysis

An unbiased stereological estimation of dopamine neurons immunolabeled with TH, total number of neurons immunolabeled with NeuN, and oligodendrocytes immunolabeled with APC was performed with an optical fractionator as previously described (Mayhew and Gundersen, 1996). The sections used for counts covered the entire substantia nigra from the rostral tip of the pars compacta back to the caudal end of the pars reticulate. This generally yielded eight to nine sections in a series. Sampling was performed with the Olympus CAST-Grid system (Olympus Denmark A/S, Denmark), with an Olympus BX51 microscope connected to the stage and feeding the computer with distance information in the z-axis. The region of interest was delineated with a 1.25× objective. A counting frame (60%, 35,650 μm^2) was placed randomly on the first counting area and systemically moved through all counting areas until the entire delineated area had been sampled. Actual counting was performed with a 40× oil objective. Guard volumes (4 μm from the top and 4–6 μm from the bottom of the section) were excluded from both surfaces to avoid the problem of lost caps, and only the profiles that came into focus within the counting volume (with a depth of 10 μm) were counted. The total number of cells was calculated according to the optical fractionator formula (West et al., 1991).

Pole Test and Grip Strength Test

For the pole test, animals were placed head upward on top of a vertical wooden pole 50 cm long and 1 cm in diameter. The base of the pole was placed in the home cage. When placed on the pole, animals orient themselves downward and descend the length of the pole back into their home cage. Groups of mice received 2 days of training that consisted of five trials for each session. On the test day, animals received five trials, and total time to descend (T-Total) was measured.

In order to ascertain peak grip strength, the animals were allowed to grasp a grid connected to an isometric dynamometer (Bioseb) and slowly moved backward until they released it for three consecutive trials. The peak strength was expressed in grams.

Statistical Analysis

Statistical analyses were performed by commercially available software (SPSS version 10.0; SPSS, Chicago, IL). Group means were compared by the Mann-Whitney *U*-test for pairs and the Kruskal-Wallis analysis for multiple groups. Behavioural changes resulting from 3NP treatment were analyzed by nonparametric paired *t*-tests. Statistical significance was deemed to be $P < 0.05$.

Results

3NP Induces αsyn Posttranslational Modifications in MBP-hαsyn Mice

In order to investigate effect of 3NP administration on αsyn, brain homogenates from vehicle- and 3NP-treated MBP-hαsyn mice and age-matched NTg controls were fractionated to obtain buffer-soluble (TBS), detergent-soluble (SDS), and detergent-insoluble (urea) fractions with each fraction represent increasing insolubility of αsyn. Immunoblot analysis of each of these fractions was conducted (Fig. 1A), and levels of nitrated asyn (Fig. 1A–D), oxidized αsyn (Fig. 1A,E–G), phosphorylated αsyn (Fig. 1A,H–J), and total αsyn (Fig. 1A,K–M) were examined.

Analysis of the levels of nitrated αsyn in each fraction revealed a significant increase in the vehicle- and 3NP-treated MBP-hαsyn mice in comparison to the vehicle- or 3NP-treated NTg mice in the SDS fraction (Figs. 1A,C and 2A) and in the 3NP-treated MBP-hαsyn mice in comparison to the vehicle-treated MBP-hαsyn and vehicle- or 3NP-treated NTg mice in the urea fraction (Figs. 1A,D and 2A). Interestingly, analysis of the TBS fraction (Figs. 1A,B and 2A), representing more soluble proteins, revealed a different distribution of nitrated αsyn; here, the 3NP-treated MBP-hαsyn mice expressed significantly lower levels of nitrated αsyn in comparison to vehicle-treated MBP-hαsyn mice and vehicle- and 3NP-treated NTg mice. 3NP administration had no significant effect on the levels of nitrated αsyn expression in the vehicle or 3NP-treated NTg mice in the TBS, SDS, or urea fractions (Figs. 1A,B–D and 2A).

Analysis of the levels of oxidized αsyn in each fraction revealed a significant increase in the levels of oxidized αsyn in the 3NP-treated MBP-hαsyn mice in comparison to the vehicle-treated MBP-hαsyn mice or 3NP-treated NTg mice in the SDS fraction (Figs. 1A,F and 2B) and in the vehicle- and 3NP-treated MBP-hαsyn mice in comparison to the vehicle- or 3NP-treated NTg mice in the urea fraction (Figs. 1A,G and 2B). 3NP administration also significantly increased the levels of oxidized αsyn in the urea fraction of the NTg mice in comparison to vehicle-treated NTg mice (Figs. 1A,G and 2B). In the TBS fraction, 3NP treatment significantly increased the levels of oxidized αsyn in the NTg mice in comparison to vehicle-treated NTg mice (Figs. 1A,E and 2B). Analogous to the results with nitrated αsyn in the TBS fraction, levels of oxidized αsyn in the vehicle- and 3NP-treated MBP-hαsyn mice were significantly lower in the TBS fraction in comparison to vehicle- and 3NP-treated NTg mice.

Immunoblot analysis of phosphorylated and total αsyn (Fig. 1A) revealed expected higher levels of phosphorylated and total αsyn in MBP-hαsyn mice in comparison to NTg mice, as has been previously reported (Shults et al., 2005;Ubhi et al., 2008). Levels of phosphorylated and total αsyn in the TBS, SDS, and urea fractions of the MBP-hαsyn mice were unchanged by 3NP administration in comparison to vehicle-treated MBP-hαsyn mice (Figs. 1A,H–J and 2C). 3NP-treated NTg mice displayed a decrease in expression levels of phosphorylated αsyn in comparison to vehicle-treated NTg mice in the TBS fraction (Figs. 1A,H and 2C) but an increase in the urea fraction (Figs. 1A,H and 2C). 3NP administration had no effect on levels of total αsyn expression in the NTg or the MBP-hαsyn mice (Figs. 1A,K–M and 2D).

Challenge With 3NP Increases Oligodendroglial Accumulation of αsyn in MBP-hαsyn Mice

Immunohistochemical analysis of the basal ganglia and frontal cortex was performed with antibodies against nitrated (Fig. 3), phosphorylated (Fig. 4), and total (Fig. 5) hαsyn in order to ascertain the effects of 3NP on the oligodendrocytic expression of αsyn in MBP-hαsyn mice. Oligodendrocytes were identified on the basis of their morphology. Analysis of the basal ganglia revealed that 3NP treatment resulted in a significant increase in nitrated αsyn immunoreactivity in the oligodendrocytes of MBP-hαsyn mice in comparison to both vehicle-treated MBP-hαsyn mice and vehicle- and 3NP-treated NTg mice (Fig. 3A–D, analyzed in E). Analysis of nitrated αsyn immunoreactivity in the frontal cortex revealed a similar pattern to that seen in the basal ganglia with the 3NP-treated MBP-hαsyn mice displaying significantly higher oligodendrocytic nitrated αsyn immunoreactivity in comparison to both vehicle-treated MBP-hαsyn mice and vehicle- and 3NP-treated NTg mice (Fig. 3F–I, analyzed in J). 3NP treatment had no effect on nitrated αsyn immunoreactivity in NTg mice in either region examined.

Immunohistochemical analysis of phosphorylated αsyn immunoreactivity in the basal ganglia (Fig. 4A–E) and frontal cortex (Fig. 4F–J) revealed that, as expected, MBP-hαsyn mice displayed significantly higher phosphorylated-αsyn (pSer159) immunoreactivity in these regions in comparison to NTg mice (Fig. 4A,C,F,H, analyzed in E and J). 3NP treatment had no significant effect on levels of phosphorylated-αsyn immunoreactivity in MBP-hαsyn or NTg mice in either region examined (Fig. 4B,D,G,I analyzed in E and J).

Analysis of human αsyn immunoreactivity revealed significantly increased αsyn immunoreactivity in the oligodendrocytes of 3NP-treated MBP-hαsyn mice in comparison to vehicle-treated MBP-hαsyn mice in both the basal ganglia and frontal cortex. 3NP treatment had no effect on human αsyn oligodendrocytic immunoreactivity in NTg mice in either region (Fig. 5A–D, analyzed in E, and F–I, analyzed in J).

3NP Administration Induces Caspase 3 Activation in a Subset of Oligodendrocytes and Neurons in the MBP-hαsyn Mice

In an order to investigate the combined effects of αsyn expression and 3NP treatment on the levels of neurodegeneration double labeling, immunohistochemical analysis was performed to examine the expression levels of activated caspase 3 and αsyn in the frontal cortex.

Significantly higher levels of caspase 3 activation were observed in the vehicle-treated MBP-hαsyn mice in comparison to the vehicle-treated NTg mice (Fig. 6D,H). 3NP administration dramatically increased this caspase 3 activation in the MBP-hαsyn mice (Fig. 6G,J) and to a more modest extent in the NTg mice (Fig. 6A,D).

Analysis of the relative expression of active caspase 3 between neurons and oligodendrocytes (on the basis of their morphology) revealed significantly higher immunoreactivity for caspase 3 in the neurons of 3NP-treated MBP-hαsyn mice in comparison to vehicle-treated MBP-

hαsyn mice (Fig. 6M), with neurons from vehicle-treated MBP-hαsyn mice themselves displaying much higher levels of caspase 3 activation than vehicle-treated NTg mice. Oligodendrocytic caspase activation was also significantly higher in the 3NP-treated MBP-hαsyn mice in comparison to vehicle-treated MBP-hαsyn mice (Fig. 6M). There was minimal active caspase 3 immunoreactivity in the oligodendroglia from vehicle-or 3NP-treated NTg mice. Thus, although 3NP treatment lead to an increase in neuronal caspase 3 activation in both the 3NP-treated NTg and MBP-hαsyn mice, an increase in oligodendrocytic caspase activation was only observed in the MBP-hαsyn mice (Fig. 6M).

3NP induced oligodendrocytic expression of activated caspase 3, and in addition, colocalization of the active caspase 3 signal with the αsyn signal in a subset of cells in the MBP-hαsyn mice in comparison to the vehicle-treated MBP-hαsyn mice (Fig. 6L, arrow). In contrast, no colocalization between caspase 3 activation and αsyn expression was observed in the vehicle-treated MBP-hαsyn mice (Fig. 6I).

3NP Treatment Exacerbates Behavioral Deficits in MBP-hαsyn Mice

In order to assess whether the posttranslational αsyn modifications induced by 3NP administration had any behavioral consequences, vehicle- and 3NP-treated NTg and MBP-hαsyn mice were analyzed by the pole test, which has been linked to basal ganglia function (Matsuura et al., 1997) and has previously been used to demonstrate behavioral impairments in MBP-hαsyn mice (Shults et al., 2005). 3NP-treated MBP-hαsyn mice took significantly longer to complete the pole test than both vehicle-treated MBP-hαsyn mice and vehicle-and 3NP-treated NTg mice (Fig. 7A). These results are consistent with the immunohistochemical analysis of the basal ganglia. 3NP administration also appeared to increase the time taken by NTg mice to complete that test in comparison to vehicle-treated NTg mice. However, this did not reach statistical significance as a result of the degree of performance variability in the 3NP-treated NTg mice (Fig. 7A).

In the grip test (Fig. 7B), there was a significant decrease in grip strength in 3NP-treated MBP-hαsyn mice in comparison to both vehicle-treated MBP-hαsyn mice and vehicle- and 3NP-treated NTg mice. There was a trend toward decreased grip strength in the vehicle-treated MBP-hαsyn mice in comparison to vehicle-treated NTg mice ($P = 0.063$), and 3NP-treated NTg mice also displayed a trend toward decreased grip strength in comparison to vehicle-treated NTg mice ($P = 0.063$).

3NP Administration Induces Widespread Degeneration in MBP-hαsyn Mice

In order to evaluate the wider effects of the 3NP-induced increases in oligodendrocytic αsyn accumulation, we examined degenerative alterations in neuronal and oligodendrocytic cells. Analysis of the substantia nigra revealed a significant loss of dopaminergic neurons, as assessed by TH immunoreactivity, in the 3NP-treated MBP-hαsyn mice in comparison to both vehicle-treated MBP-hαsyn mice and vehicle- and 3NP-treated NTg mice. Vehicle-treated MBP-hαsyn mice themselves displayed decreased TH immunoreactivity in comparison to vehicle-treated NTg, indicating lower basal levels of dopaminergic neurons in the transgenic mice. 3NP administration also decreased TH immunoreactivity in NTg mice in comparison to vehicle-treated NTg mice (Fig. 8A–E).

Analysis of neuronal number, as assessed by NeuN immunoreactivity in the striatum (Fig. 8F–J) and frontal cortex (Fig. 8K–O), revealed a similar pattern. 3NP-treated MBP-hαsyn mice displayed lower NeuN immunoreactivity in both these regions in comparison to both vehicle-treated MBP-hαsyn mice and vehicle- and 3NP-treated NTg mice (Fig. 8J,O). 3NP administration also resulted in a decreased in neuronal density in the striatum and frontal cortex of NTg mice in comparison to vehicle-treated NTg mice (Fig. 8J,O).

Immunohistochemical analysis was also performed in order to assess the effect of 3NP administration on oligodendroglial pathology. Analysis of the corpus callosum and cerebellar white matter, key regions implicated in MSA pathology, revealed decreases in APC immunoreactivity in both regions in vehicle-treated MBP-hαsyn mice in comparison to vehicle-treated NTg mice (Fig. 9A,C and F,H, analyzed in E and J). 3NP administration significantly decreased APC immunoreactivity in the corpus callosum of MBP-hαsyn mice in comparison to vehicle-treated MBP-hαsyn mice (Fig. 9C–E) but had no significant effect on APC immunoreactivity in the cerebellar white matter of the MBP-hαsyn mice. 3NP administration had no effect on APC immunoreactivity in the corpus callosum of the NTg mice (Fig. 9B,D,E). However, there was a significant decrease in APC immunoreactivity in the cerebellar white matter of 3NP-treated NTg mice in comparison to vehicle-treated NTg mice (Fig. 9F,G,J).

Results from neuro- and oligopathological analysis of 3NP administration revealed decreased neuronal and oligodendroglial density in a number of regions associated with MSA. These results are consistent with previous studies that have examined the effect of 3NP in mouse models of MSA (Stefanova et al., 2005a).

Discussion

The present study examined the effects of oxidative stress, as induced by the mitochondrial inhibitor 3NP, on posttranslational modifications of αsyn and on the effects of these modifications on pathology and behavior. The results presented herein demonstrate that 3NP administration led to oxidation-specific modifications of αsyn that were concomitant with an exacerbation of behavioral deficits and widespread neuronal and oligodendrocytic pathology in a number of brain regions implicated in MSA (Wenning et al., 2008).

Our work follows on closely from the work of Stefanova et al. (2005a), who have previously described 3NP-induced intensification of neuropathology and behavioral deficits in a mouse model of MSA. However, the present work differs from the aforementioned study in a number of important aspects. First, the present study uses a different mouse model of MSA. A number of transgenic mouse models currently exist that model the neuropathological features of MSA to various degrees (Kahle et al., 2002; Shults et al., 2005; Stefanova et al., 2005b; Yazawa et al., 2005). The present study was conducted in a model wherein the expression of αsyn has been targeted to the oligodendrocytes by virtue of the MBP promoter. This model has been extensively characterized and has previously been shown to result in extensive accumulation of αsyn and severe neuropathological alteration in the neocortex, basal ganglia, and cerebellum, key structures responsible for neurological deficits in patients with MSA (Shults et al., 2005). Second, this study uses a 3NP dosing regimen that differs in timing and concentration from the previous study, avoiding the lethal toxicity effects that were reported with higher doses of 3NP. Third, the present study, while addressing the effects of 3NP on pathology and behavior, focuses mainly on αsyn itself and how it is modified on 3NP administration.

Our results indicate that administration of 3NP results in oxidative modifications to αsyn, as evidenced by the immunoblot and immunohistochemical analysis of nitrated and oxidized αsyn. The immunoblot data appear to demonstrate a shift of the nitratively and/or oxidatively modified forms of αsyn from the TBS to SDS or urea fractions, which indicates that these modifications in the MBP-hαsyn mice may result in reduced αsyn solubility. In contrast, levels of phosphorylated and total αsyn remain largely unaffected by 3NP administration, indicating a specificity of 3NP-induced posttranslational modification rather than global effects on αsyn.

The overexpression of human αsyn alone has been shown to induce behavioral deficits and neurodegeneration (Hashimoto et al., 2003; Kahle, 2008). However, modifications such as

phosphorylation and oxidative/nitrative modifications have been shown to increase the fibrillogenesis, aggregation, and toxicity of αsyn (Beyer, 2006; Norris and Giasson, 2005; Norris et al., 2003), although the precise role and importance of each modification in this toxicity are still unclear. Although phosphorylation of αsyn (particularly at S129) has been previously linked to αsyn toxicity and a possible protective role via inclusion formation in *Drosophila* (Chen and Feany, 2005), its exact role is still unclear, and recent studies that use αsyn mutants in which phosphorylation has been constitutively inhibited (S129A) or activated (S129D) to tease out the importance of phosphorylation in rodents have shown that phosphorylation at S129 is not necessary to induce pathology (Gorbatyuk et al., 2008) and have called into question the proposed protective role of inclusion formation by demonstrating activation of apoptotic markers after inclusion formation by the αsyn phosphorylation mimicking S129D mutants (Azeredo da Silveira et al., 2009). In contrast, nitrative and oxidative modifications of alpha synuclein have been more consistently reported to be involved in the fibrillogenesis and aggregation of alpha synuclein, resulting in the formation of SDS-soluble alpha synuclein (Norris et al., 2003). It is unlikely that one single modification alone is responsible for the behavioral and pathological changes seen in models of alpha-synucleinopathies. Rather, the presence of all these modification in the brains of patients diagnosed with Parkinson's disease, Lewy body disease, and MSA (Burn and Jaros, 2001; Duda et al., 2000a, 2000b; Giasson et al., 2000; Gomez-Tortosa et al., 2002; Ischiropoulos, 2003; Jenner, 1996; Kikuchi et al., 2002; Norris and Giasson, 2005) suggests that they work in conjunction to lead to neurodegeneration.

Because the observation that abnormally aggregated and posttranslationally modified αsyn forms a major component of the inclusions observed in MSA (Burn and Jaros, 2001; Duda et al., 2000b; Kikuchi et al., 2002; Tu et al., 1998; Yamashita et al., 2000), and other αsyn nucleopathies (Duda et al., 2000a; Giasson et al., 2000; Gomez-Tortosa et al., 2002; Kikuchi et al., 2002; Waxman et al., 2008), much research has been focused on trying to elucidate the mechanisms that underlie the transformation of this natively unfolded and soluble protein into the insoluble form found in these aggregates. Oxidative stress has been proposed as a possible mechanism that may link αsyn posttranslational modifications to subsequent aggregation (Bieschke et al., 2006; Ischiropoulos, 2003; Jenner, 1996; Maguire-Zeiss et al., 2005; Norris and Giasson, 2005; Schapira, 2008). A recent study (Mirzaei et al., 2006) examining the effects of rotenone, a mitochondrial complex I inhibitor, on a C-terminal 20-residue stretch of αsyn, revealed multiple modifications on five specific residues (M116, Y125, M127, Y133, and Y136), including phosphorylation, nitration, and amination. Interestingly, each residue demonstrated a number of possible modifications upon exposure to rotenone, but not all residues demonstrated the same propensity for different modifications; for instance, Y125 could be phosphorylated, nitrated, or aminated, whereas Y133 was shown to be nitrated or aminated but never phosphorylated. These results demonstrate that these αsyn residues are highly susceptible to oxidative modification and that oxidative stress can result in a number of different modifications. The impact of oxidative stress on αsyn aggregation was demonstrated by a study (Norris et al., 2003) in which exposure to nitrative ($ONOO^-$, peroxynitrite) or oxidative (H_2O_2 and/or transition metals such as copper) stresses was shown to stabilize the formation of αsyn dimers and oligomers by the formation of covalent dityrosine crosslinks. Interestingly, this study showed that the presence of Tyr residues (Y39, 125, 133, and 136) was required for the cross-linking induced by $ONOO^-$, but not by H_2O_2 and/or transition metals. The authors of this work also report that αsyn fibrillogenesis in response to nitrating agents was dependent on the presence of the tyrosine residues, whereas that in response oxidizing agents was not. Collectively, the results from this study suggest that divergent mechanisms underlie the pathogenesis of nitrative and oxidative insults.

The results from this study indicate that 3NP administration may parody the pathological effects of oxidative stress in MSA, with 3NP-treated MBP-hαsyn tg mice mimicking the

neuropathological characteristics of human MSA and also expressing oxidatively modified αsyn species as reported in MSA. Interestingly, 3NP treatment also has effects on the NTg mice. This may be because of its actions on the endogenous αsyn present in these mice. Experiments in αsyn knockout mice are under way to address this issue. Caspase activation in a subset of oligodendrocytes that express αsyn indicates that these cells are apoptotic; interestingly, caspase activation in the neurons surrounding the αsyn expressing oligodendrocytes suggests that these neurons may be also be experiencing some ill effect of the oligodendrocytic accumulation of αsyn, perhaps as a result of a lack of trophic support being provided by the damaged oligodendrocytes.

It remains to be determined whether oxidative stress is a cause, result, or epiphenomenon of the disease process in MSA, or whether oxidatively modified αsyn form the primary toxic species or are one of a number or modifications, such as αsyn cleavage (Dufty et al., 2007; Kasai et al., 2008; Mishizen-Eberz et al., 2005), that underlie the pathogenesis observed in MSA. Ongoing and future research into MSA needs to be aimed at unraveling the interactions between oxidative stress and asyn modifications and aggregation. In light of the fact that direct genetic causes of MSA remain elusive, the current models of MSA focus on the oligodendrocytic expression of αsyn. However, the administration of 3NP and the induction of oxidative stress in these animals provide a model in which to examine the pathological consequences after the coincident induction of these factors. The results from this and from previous studies (Stefanova et al., 2005a) suggest that 3NP administration in MBP-hαsyn tg mice may provide a useful model in which to further investigate the complex relationships between oxidative stress, αsyn modification, and the subsequent pathogenesis observed in MSA.

Acknowledgments

This work was funded by NIH grants AG18440, NS044233, and AG 022074.

References

Azeredo da Silveira S, Schneider BL, Cifuentes-Diaz C, Sage D, Abbas-Terki T, Iwatsubo T, Unser M, Aebischer P. Phosphorylation does not prompt, nor prevent, the formation of alpha-synuclein toxic species in a rat model of Parkinson's disease. Hum Mol Genet 2009;18:872–887. [PubMed: 19074459]

Beyer K. Alpha-synuclein structure, posttranslational modification and alternative splicing as aggregation enhancers. Acta Neuropathol 2006;112:237–251. [PubMed: 16845533]

Bieschke J, Zhang Q, Bosco DA, Lerner RA, Powers ET, Wentworth P Jr, Kelly JW. Small molecule oxidation products trigger disease-associated protein misfolding. Acc Chem Res 2006;39:611–619. [PubMed: 16981677]

Burn DJ, Jaros E. Multiple system atrophy: cellular and molecular pathology. Mol Pathol 2001;54:419–426. [PubMed: 11724918]

Chen L, Feany MB. Alpha-synuclein phosphorylation controls neurotoxicity and inclusion formation in a *Drosophila* model of Parkinson disease. Nat Neurosci 2005;8:657–663. [PubMed: 15834418]

Duda JE, Giasson BI, Chen Q, Gur TL, Hurtig HI, Stern MB, Gollomp SM, Ischiropoulos H, Lee VM, Trojanowski JQ. Widespread nitration of pathological inclusions in neurodegenerative synucleinopathies. Am J Pathol 2000a;157:1439–1445. [PubMed: 11073803]

Duda JE, Giasson BI, Gur TL, Montine TJ, Robertson D, Biaggioni I, Hurtig HI, Stern MB, Gollomp SM, Grossman M, Lee VM, Trojanowski JQ. Immunohistochemical and biochemical studies demonstrate a distinct profile of alpha-synuclein permutations in multiple system atrophy. J Neuropathol Exp Neurol 2000b;59:830–841. [PubMed: 11005264]

Dufty BM, Warner LR, Hou ST, Jiang SX, Gomez-Isla T, Leenhouts KM, Oxford JT, Feany MB, Masliah E, Rohn TT. Calpain-cleavage of alpha-synuclein: connecting proteolytic processing to disease-linked aggregation. Am J Pathol 2007;170:1725–1738. [PubMed: 17456777]

Giasson BI, Duda JE, Murray IV, Chen Q, Souza JM, Hurtig HI, Ischiropoulos H, Trojanowski JQ, Lee VM. Oxidative damage linked to neurodegeneration by selective alpha-synuclein nitration in synucleinopathy lesions. Science 2000;290(5493):985–989. [PubMed: 11062131]

Gomez-Tortosa E, Gonzalo I, Newell K, Garcia Yebenes J, Vonsattel P, Hyman BT. Patterns of protein nitration in dementia with Lewy bodies and striatonigral degeneration. Acta Neuropathol 2002;103:495–500. [PubMed: 11935266]

Gorbatyuk OS, Li S, Sullivan LF, Chen W, Kondrikova G, Manfredsson FP, Mandel RJ, Muzyczka N. The phosphorylation state of Ser-129 in human alpha-synuclein determines neurodegeneration in a rat model of Parkinson disease. Proc Natl Acad Sci U S A 2008;105:763–768. [PubMed: 18178617]

Hanna PA, Jankovic J, Kirkpatrick JB. Multiple system atrophy: the putative causative role of environmental toxins. Arch Neurol 1999;56:90–94. [PubMed: 9923766]

Hashimoto M, Rockenstein E, Masliah E. Transgenic models of alpha-synuclein pathology: past, present, and future. Ann N Y Acad Sci 2003;991:171–188. [PubMed: 12846986]

Ischiropoulos H. Oxidative modifications of alpha-synuclein. Ann N Y Acad Sci 2003;991:93–100. [PubMed: 12846977]

Jenner P. Oxidative stress in Parkinson's disease and other neurodegenerative disorders. Pathol Biol (Paris) 1996;44:57–64. [PubMed: 8734302]

Kahle PJ. alpha-Synucleinopathy models and human neuropathology: similarities and differences. Acta Neuropathol 2008;115:87–95. [PubMed: 17932682]

Kahle PJ, Neumann M, Ozmen L, Muller V, Jacobsen H, Spooren W, Fuss B, Mallon B, Macklin WB, Fujiwara H, Hasegawa M, Iwatsubo T, Kretzschmar HA, Haass C. Hyperphosphorylation and insolubility of alpha-synuclein in transgenic mouse oligodendrocytes. EMBO Rep 2002;3:583–588. [PubMed: 12034752]

Kasai T, Tokuda T, Yamaguchi N, Watanabe Y, Kametani F, Nakagawa M, Mizuno T. Cleavage of normal and pathological forms of alpha-synuclein by neurosin in vitro. Neurosci Lett 2008;436:52–56. [PubMed: 18358605]

Kikuchi A, Takeda A, Onodera H, Kimpara T, Hisanaga K, Sato N, Nunomura A, Castellani RJ, Perry G, Smith MA, Itoyama Y. Systemic increase of oxidative nucleic acid damage in Parkinson's disease and multiple system atrophy. Neurobiol Dis 2002;9:244–248. [PubMed: 11895375]

Maguire-Zeiss KA, Short DW, Federoff HJ. Synuclein, dopamine and oxidative stress: co-conspirators in Parkinson's disease? Brain Res Mol Brain Res 2005;134:18–23. [PubMed: 15790526]

Matsuura K, Kabuto H, Makino H, Ogawa N. Pole test is a useful method for evaluating the mouse movement disorder caused by striatal dopamine depletion. J Neurosci Methods 1997;73:45–48. [PubMed: 9130677]

Mayhew TM, Gundersen HJ. If you assume, you can make an ass out of u and me": a decade of the disector for stereological counting of particles in 3D space. J Anat 1996;188(Pt 1):1–15. [PubMed: 8655396]

Mirzaei H, Schieler JL, Rochet JC, Regnier F. Identification of rotenone-induced modifications in alpha-synuclein using affinity pulldown and tandem mass spectrometry. Anal Chem 2006;78:2422–2431. [PubMed: 16579629]

Mishizen-Eberz AJ, Norris EH, Giasson BI, Hodara R, Ischiropoulos H, Lee VM, Trojanowski JQ, Lynch DR. Cleavage of alpha-synuclein by calpain: potential role in degradation of fibrillized and nitrated species of alpha-synuclein. Biochemistry 2005;44:7818–7829. [PubMed: 15909996]

Nee LE, Gomez MR, Dambrosia J, Bale S, Eldridge R, Polinsky RJ. Environmental–occupational risk factors and familial associations in multiple system atrophy: a preliminary investigation. Clin Auton Res 1991;1:9–13. [PubMed: 1821673]

Norris EH, Giasson BI. Role of oxidative damage in protein aggregation associated with Parkinson's disease and related disorders. Antioxid Redox Signal 2005;7:672–684. [PubMed: 15890012]

Norris EH, Giasson BI, Ischiropoulos H, Lee VM. Effects of oxidative and nitrative challenges on alpha-synuclein fibrillogenesis involve distinct mechanisms of protein modifications. J Biol Chem 2003;278:27230–27240. [PubMed: 12857790]

Schapira AH. Mitochondria in the aetiology and pathogenesis of Parkinson's disease. Lancet Neurol 2008;7:97–109. [PubMed: 18093566]

Shults CW, Rockenstein E, Crews L, Adame A, Mante M, Larrea G, Hashimoto M, Song D, Iwatsubo T, Tsuboi K, Masliah E. Neurological and neurodegenerative alterations in a transgenic mouse model expressing human alpha-synuclein under oligodendrocyte promoter: implications for multiple system atrophy. J Neurosci 2005;25:10689–10699. [PubMed: 16291942]

Stefanova N, Reindl M, Neumann M, Haass C, Poewe W, Kahle PJ, Wenning GK. Oxidative stress in transgenic mice with oligodendroglial alpha-synuclein overexpression replicates the characteristic neuropathology of multiple system atrophy. Am J Pathol 2005a;166:869–876. [PubMed: 15743798]

Stefanova N, Tison F, Reindl M, Poewe W, Wenning GK. Animal models of multiple system atrophy. Trends Neurosci 2005b;28:501–506. [PubMed: 16043239]

Tu PH, Galvin JE, Baba M, Giasson B, Tomita T, Leight S, Nakajo S, Iwatsubo T, Trojanowski JQ, Lee VM. Glial cytoplasmic inclusions in white matter oligodendrocytes of multiple system atrophy brains contain insoluble alpha-synuclein. Ann Neurol 1998;44:415–422. [PubMed: 9749615]

Ubhi K, Rockenstein E, Mante M, Patrick C, Adame A, Thukral M, Shults C, Masliah E. Rifampicin reduces alpha-synuclein in a transgenic mouse model of multiple system atrophy. Neuroreport 2008;19:1271–1276. [PubMed: 18695506]

Vanacore N, Bonifati V, Fabbrini G, Colosimo C, De Michele G, Marconi R, Stocchi F, Nicholl D, Bonuccelli U, De Mari M, Vieregge P, Meco G. Case–control study of multiple system atrophy. Mov Disord 2005;20:158–163. [PubMed: 15382209]

Waxman EA, Duda JE, Giasson BI. Characterization of antibodies that selectively detect alpha-synuclein in pathological inclusions. Acta Neuropathol 2008;116:37–46. [PubMed: 18414880]

Wenning GK, Colosimo C, Geser F, Poewe W. Multiple system atrophy. Lancet Neurol 2004;3:93–103. [PubMed: 14747001]

Wenning GK, Stefanova N, Jellinger KA, Poewe W, Schlossmacher MG. Multiple system atrophy: a primary oligodendrogliopathy. Ann Neurol 2008;64:239–246. [PubMed: 18825660]

West MJ, Slomianka L, Gundersen HJ. Unbiased stereological estimation of the total number of neurons in thesubdivisions of the rat hippocampus using the optical fractionator. Anat Rec 1991;231:482–497. [PubMed: 1793176]

Yamashita T, Ando Y, Obayashi K, Terazaki H, Sakashita N, Uchida K, Ohama E, Ando M, Uchino M. Oxidative injury is present in Purkinje cells in patients with olivopontocerebellar atrophy. J Neurol Sci 2000;175:107–110. [PubMed: 10831770]

Yazawa I, Giasson BI, Sasaki R, Zhang B, Joyce S, Uryu K, Trojanowski JQ, Lee VM. Mouse model of multiple system atrophy alpha-synuclein expression in oligodendrocytes causes glial and neuronal degeneration. Neuron 2005;45:847–859. [PubMed: 15797547]

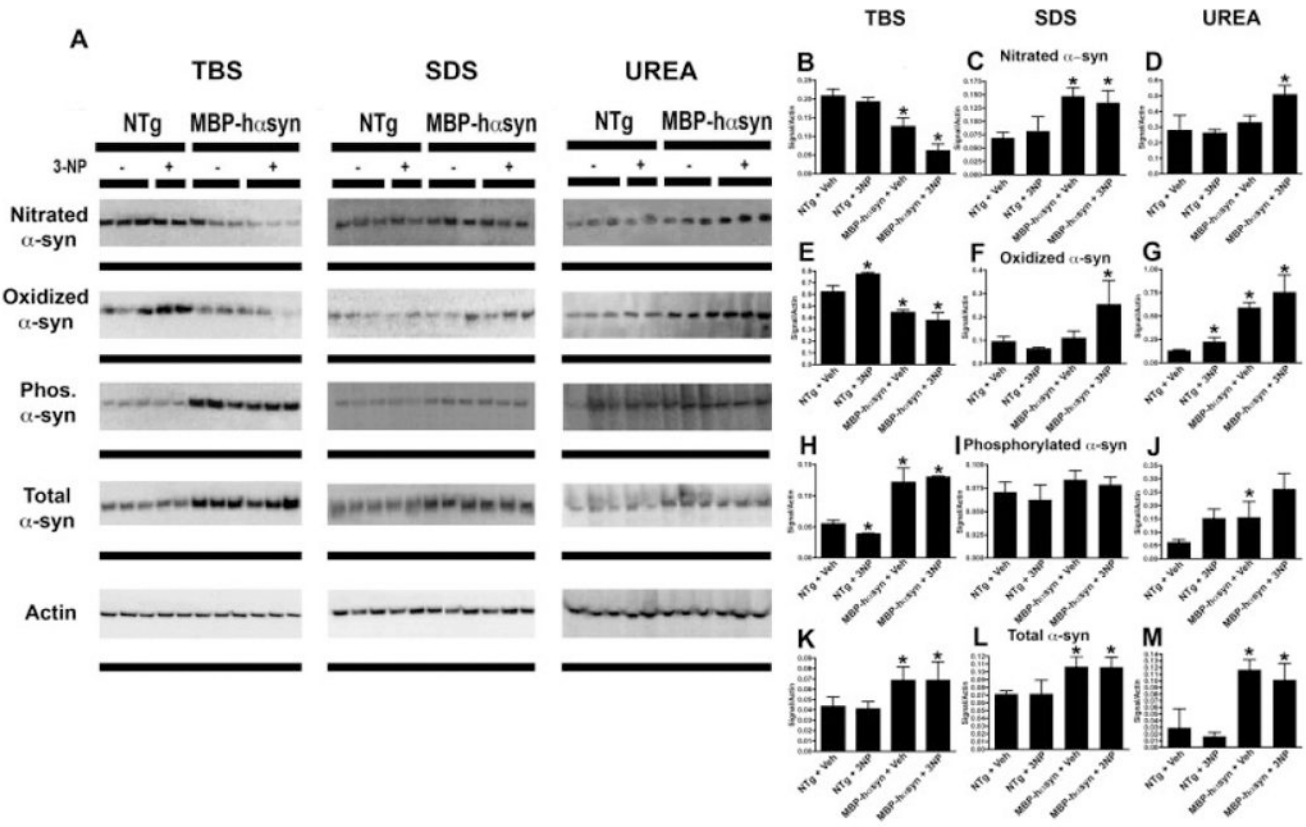

Fig. 1.

3NP-induced αsyn posttranslational modifications in MBP-hαsyn mice. Immunoblot analysis was carried out on homogenized brain samples from vehicle- and 3NP-treated NTg and MBP-hαsyn mice processed to obtain soluble (TBS), detergent-soluble (SDS), and detergent-insoluble (urea) fractions (**A**). Quantitative analysis of the blots was conducted to examine levels of nitrated αsyn in TBS (**B**), SDS (**C**), and urea (**D**) fractions, oxidized αsyn in TBS (**E**), SDS (**F**), and urea (**G**) fractions, phosphorylated αsyn in TBS (**H**), SDS (**I**), and urea (**J**) fractions, and total αsyn in TBS (**K**), SDS (**L**), and urea (**M**) fractions. Actin was used as a loading control in each case. *Significant difference ($P < 0.05$, one-way ANOVA and post hoc Fisher).

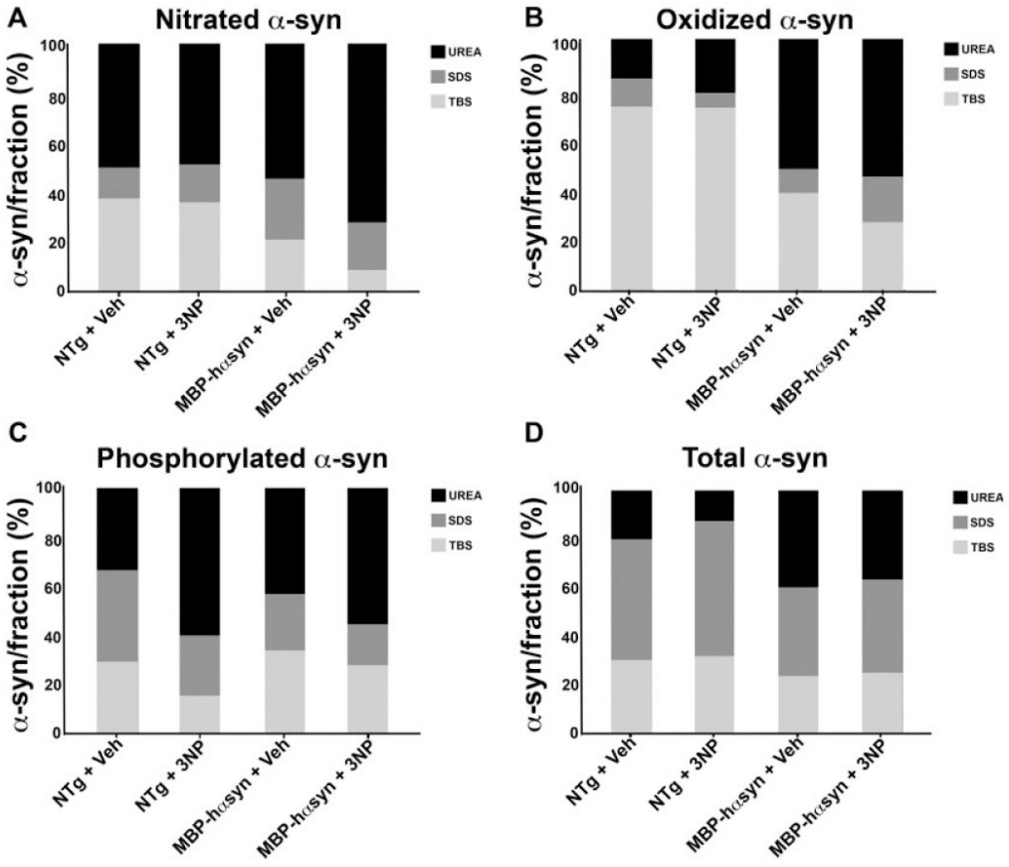

Fig. 2.

3NP-induced shift in solubility of posttranslationally modified αsyn in MBP-hasyn mice. Composite bar graphs of the levels of nitrated (**A**), oxidized (**B**), phosphorylated (**C**), and total (**D**) αsyn in the TBS, SDS, and urea fractions.

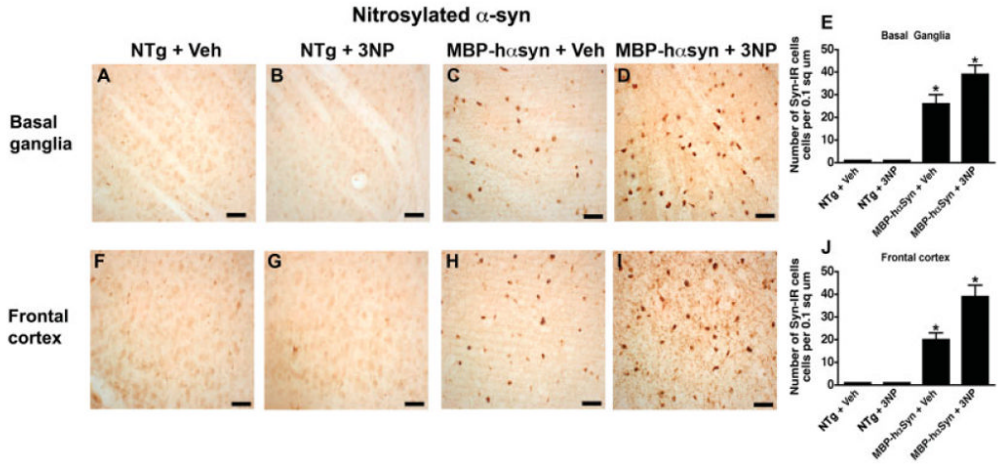

Fig. 3.

Immunohistochemical analysis of the effect of 3NP treatment on nitrated αsyn. Immunohistochemical analysis was conducted to examine the levels of nitrated αsyn in the basal ganglia of vehicle-treated NTg mice (**A**), 3NP-treated NTg mice (**B**), vehicle-treated MBP-hαsyn mice (**C**), and 3NP-treated MBP-hαsyn mice (**D**). Quantitative analysis of basal ganglia levels of nitrated αsyn (**E**). Immunohistochemical analysis was also conducted to examine the levels of nitrated αsyn in the frontal cortex of vehicle-treated NTg mice (**F**), 3NP-treated NTg mice (**G**), vehicle-treated MBP-hαsyn mice (**H**), and 3NP-treated MBP-hαsyn mice (**I**). Quantitative analysis of frontal cortical levels of nitrated αsyn (**J**). Scale bar = 50 μM. *Significant difference ($P < 0.05$, one-way ANOVA and post hoc Fisher). [Color figure can be viewed in the online issue, which is available at www.interscience. wiley.com.]

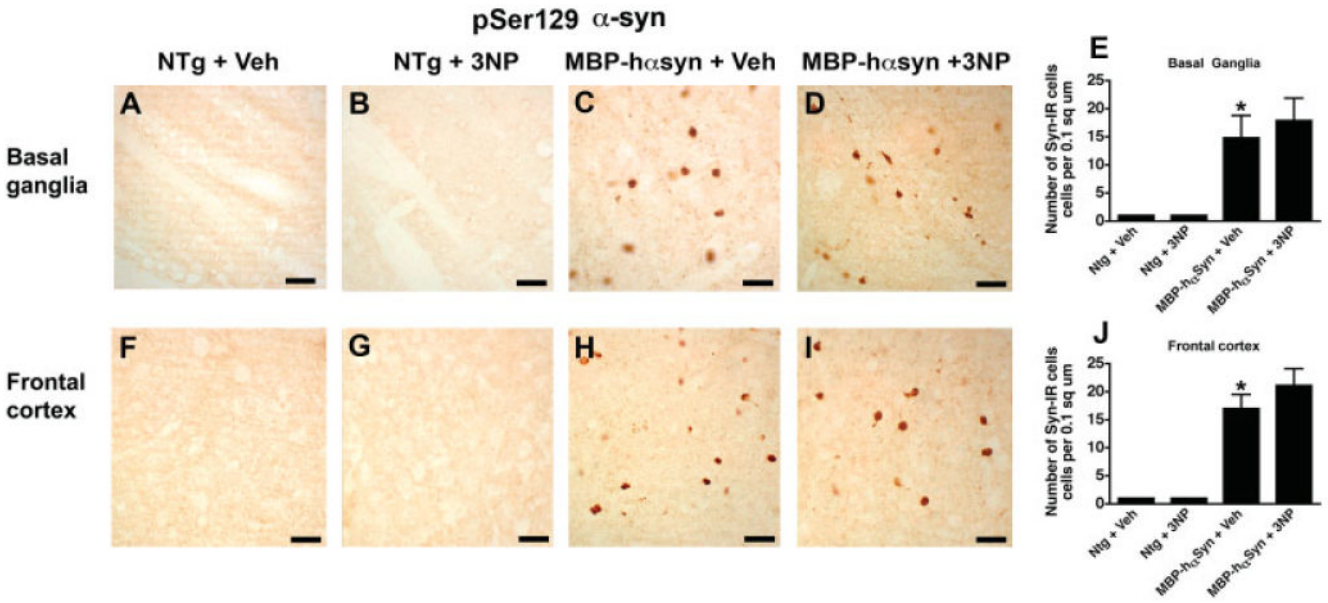

Fig. 4.

Immunohistochemical analysis of the effect of 3NP treatment on phosphorylated αsyn. Immunohistochemical analysis was conducted to examine the levels of phosphorylated αsyn in the basal ganglia of vehicle-treated NTg mice (**A**), 3NP-treated NTg mice (**B**), vehicle-treated MBP-hαsyn mice (**C**), and 3NP-treated MBP-hαsyn mice (**D**). Quantitative analysis of basal ganglia levels of phosphorylated αsyn (**E**). Immunohistochemical analysis was also conducted to examine the levels of phosphorylated αsyn in the frontal cortex of vehicle-treated NTg mice (**F**), 3NP-treated NTg mice (**G**), vehicle-treated MBP-hαsyn mice (**H**), and 3NP-treated MBP-hαsyn mice (**I**). Quantitative analysis of frontal cortical levels of phosphorylated αsyn (**J**). Scale bar = 50 μM. *Significant difference ($P < 0.05$, one-way ANOVA and post hoc Fisher). [Color figure can be viewed in the online issue, which is available at www.interscience.wiley.com.]

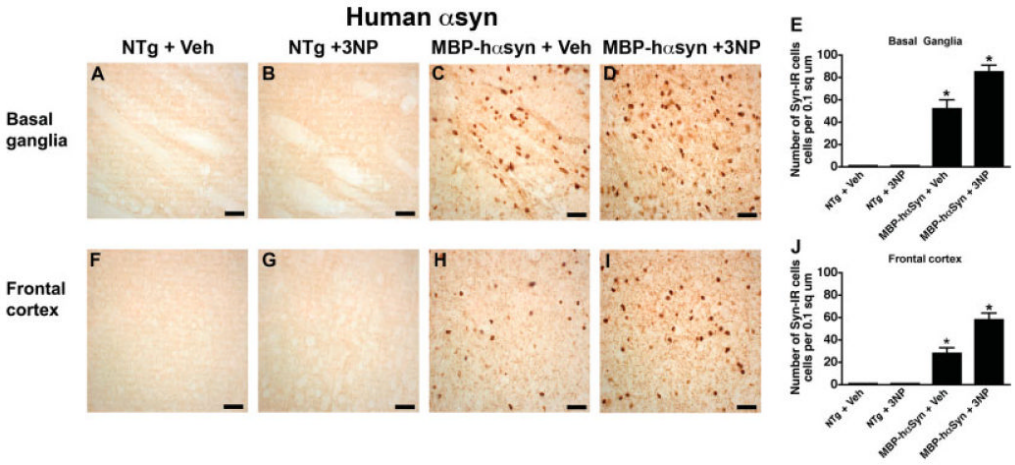

Fig. 5.

Immunohistochemical analysis of the effect of 3NP treatment on human αsyn. Immunohistochemical analysis was conducted to examine the levels of human αsyn in the basal ganglia of vehicle-treated NTg mice (**A**), 3NP-treated NTg mice (**B**), vehicle-treated MBP-hαsyn mice (**C**), and 3NP-treated MBP-hαsyn mice (**D**). Quantitative analysis of basal ganglia levels of human αsyn was also performed (**E**). Immunohistochemical analysis was also conducted to examine the levels of human αsyn in the frontal cortex of vehicle-treated NTg mice (**F**), 3NP-treated NTg mice (**G**), vehicle-treated MBP-hαsyn mice (**H**), and 3NP-treated MBP-hαsyn mice (**I**). Quantitative analysis of frontal cortical levels of human αsyn was also performed (**J**). Scale bar = 50 μm. *Significant difference ($P < 0.05$, one-way ANOVA and post hoc Fisher). [Color figure can be viewed in the online issue, which is available at www.interscience.wiley.com.]

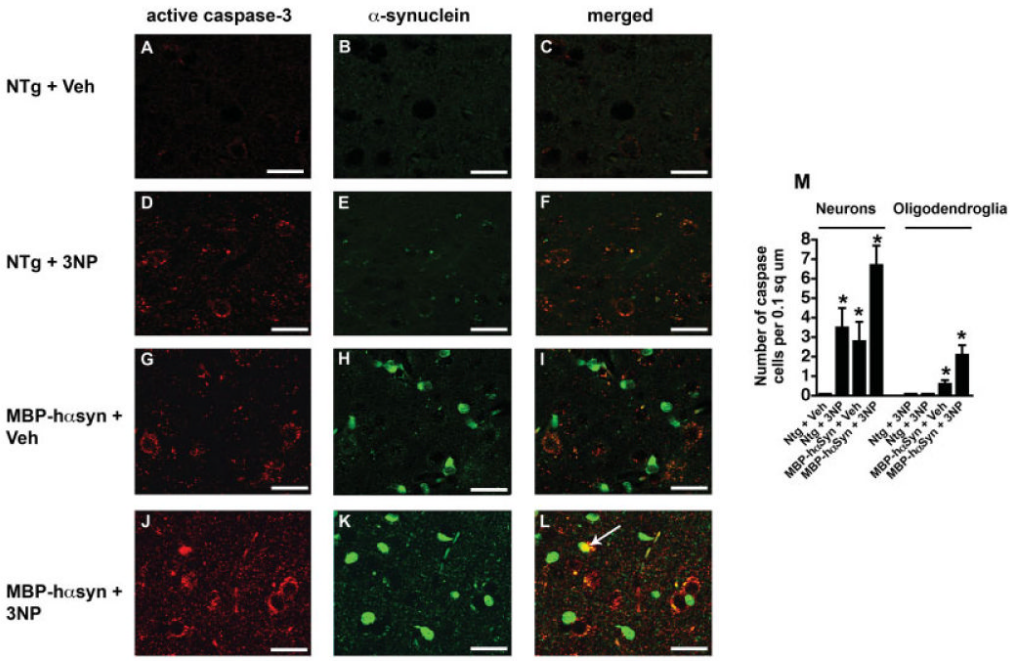

Fig. 6.

3NP treatment induced colocalization of αsyn and caspase activation in oligodendrocytes in MBP-hαsyn mice. Active caspase 3 immunoreactivity in vehicle-treated NTg mice (**A**), 3NP-treated NTg mice (**D**), vehicle-treated MBP-hαsyn mice (**G**), and 3NP-treated MBP-hαsyn mice (**J**). αsyn immunoreactivity in vehicle-treated NTg mice (**B**), 3NP-treated NTg mice (**E**), vehicle-treated MBP-hαsyn mice (**H**), and 3NP-treated MBP-hαsyn mice (**K**). Colocalization of active caspase 3 and αsyn signal in vehicle-treated NTg mice (**C**), 3NP-treated NTg mice (**F**), vehicle-treated MBP-hαsyn mice (**I**), and 3NP-treated MBP-hαsyn mice (**L**). Quantitative analysis of the levels of activated caspase 3 immunoreactive neurons and oligodendroglia in vehicle- and 3NP-treated NTg and MBP-hasyn mice (**M**). Scale bar = 50 μM.

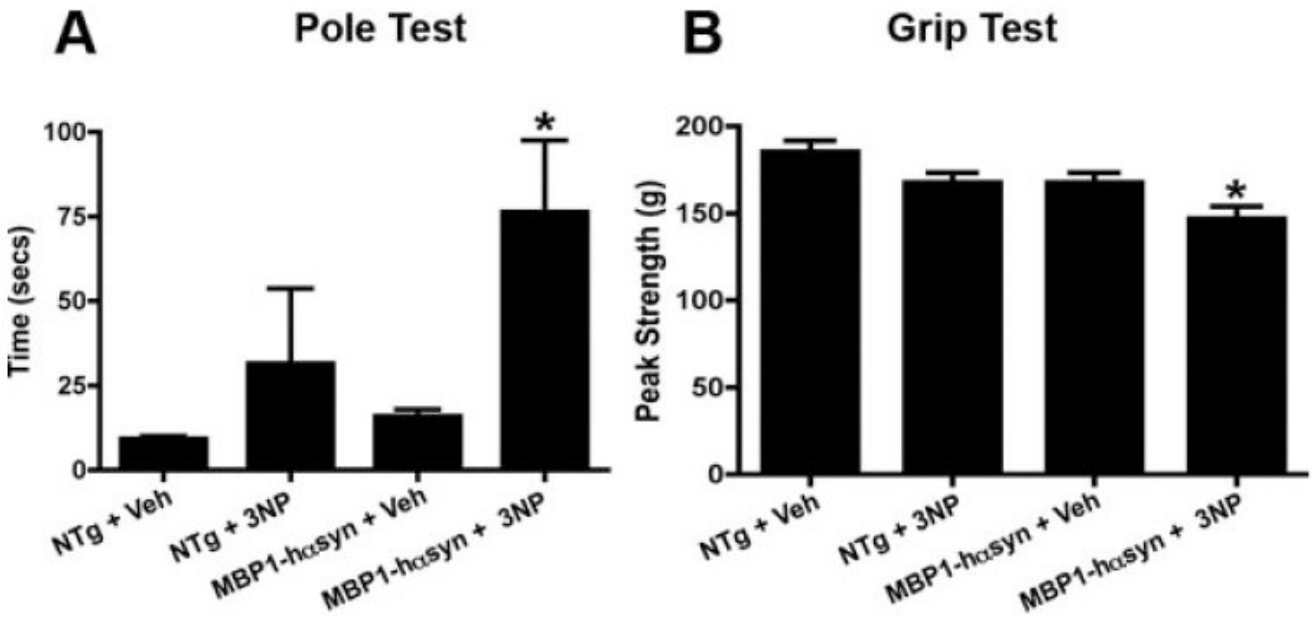

Fig. 7.

3NP treatment exacerbates behavioral deficits in MBP-hαsyn mice. Motor behavior was assessed by the pole test (**A**). Mice were placed at the top of a vertical pole, and total time to descend (T-Total) was measured. Mice received 2 days of training, five trials each day, and were analyzed on the third day. Peak grip strength (g) was assessed (**B**) in three consecutive trials by allowing the mice to grasp a grid connected to an isometric dynamometer; mice were slowly moved backward until they released the bar. *Significant difference ($P < 0.05$, one-way ANOVA and post hoc Fisher).

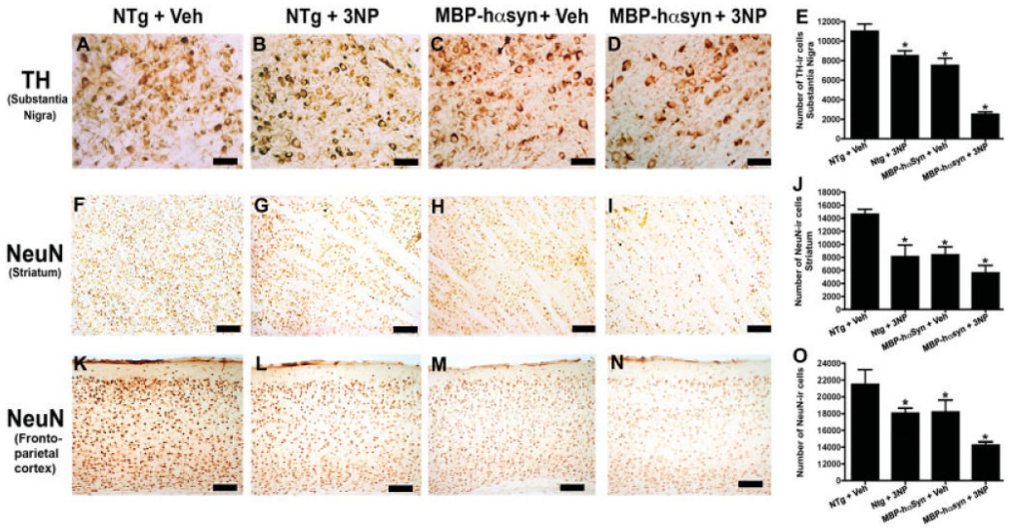

Fig. 8.

Widespread neuropathology as a result of 3NP treatment. Immunohistochemical analysis was performed to examine the number of TH-positive cells in the substantia nigra of vehicle- and 3NP-treated NTg and vehicle- and 3NP-treated MBP-hαsyn mice (**A–D**, respectively, and analyzed in **E**). Neuronal density, as determined by NeuN immunoreactivity, was analyzed the striatum of vehicle- and 3NP-treated NTg and vehicle- and 3NP-treated MBP-hasyn mice (**F–I**, respectively, and analyzed in **J**). Neuronal density was also examined in the frontoparietal cortex of vehicle- and 3NP-treated NTg and vehicle- and 3NP-treated MBP-hαsyn mice (**K–N**, respectively, and analyzed in **O**). Scale bar = 50 μM in A–D. Scale bar = 200 μM in F–I, K–N. *Significant difference ($P < 0.05$, one-way ANOVA and post hoc Fisher). [Color figure can be viewed in the online issue, which is available at www.interscience.wiley.com.]

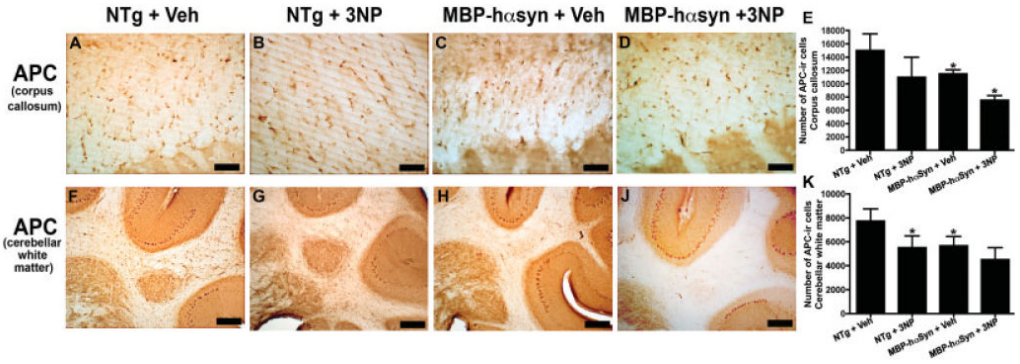

Fig. 9.

Oligodendroglial pathology as a result of 3NP treatment. In order to examine the effects of 3NP treatment on oligodendrocytes, levels of APC, an oligodendrocytic marker, were examined in the corpus callosum of vehicle- and 3NP-treated NTg and vehicle- and 3NP-treated MBP-hasyn mice (**A–D**, respectively, and analyzed in **E**). APC levels were also examined in the cerebellar white matter of vehicle- and 3NP-treated NTg and vehicle- and 3NP-treated MBP-hasyn mice (**F–I**, respectively, and analyzed in **J**). Scale bar = 200 μM. *Significant difference ($P < 0.05$, one-way ANOVA and post hoc Fisher). [Color figure can be viewed in the online issue, which is available at www.interscience.wiley.com.]